EFFECT OF THE IRON ORE ON MICROSTRUCTURAL CHANGES OF A REFRACTORY CONCRETE MAGNESIUM ALUMINATE BASE

R. Puente-Ornelas[a]*, P. C. Zambrano[a], C. Frausto-Reyes[b], E. Rodríguez[a], C. J. Lizcano-Zuláica[a], A. M. Guzmán[a], G. Trujillo-Sánchez[a], H. M. Delgadillo-Guerra[a].

[a]Universidad Autónoma de Nuevo León, Facultad de Ingeniería Mecánica y Eléctrica, A.P. 076 Suc. "F", Cd. Universitaria C.P. 66451, San Nicolás de los Garza, N.L., México.
[b]Centro de Investigaciones en Óptica, A.C., Aguascalientes, Aguascalientes, México.

*Corresponding author, e-mail: ropuor@gmail.com, phone: +052 81-83-29-40-20, ext. 5914.

Recibido: Septiembre 2011. Aprobado: Febrero 2012.
Publicado: Febrero 2012.

ABSTRACT
In this study, it was evaluated the chemical interaction between iron ore (Fe_2O_3) and a refractory concrete based on Al_2O_3-$MgAl_2O_4$ at 1650 °C for 4 h using an air atmosphere, in order to determine the chemical behavior and possible reactions between these materials. After testing, the refractory concrete was microstructurally characterized by optical microscopy and scanning electron microscopy (SEM-EDS), as well as X-ray diffraction and Raman spectroscopy. The results showed that magnesium aluminate phase incorporates in solid solution Fe^{+2} ions, resulting in the formation of (Fe, Mg) (Al_2O_4) spinels and after their saturation, the rest of Fe^{+2} ions tends to precipitate at the grain boundaries of alumina and magnesium aluminate phases. This fact promotes during the concrete cooling, the formation of wustite, hematite and magnetite phases (detected in the microstructure as a dendritic and widmanstätten morphologies). The presence of hematite phase was corroborated by X-ray diffraction; likewise the presence of modified spinel phase whose hkl reflections width is higher compared with the original spinel, due to the incorporation of Fe^{+2} in the initial $MgAl_2O_4$ phase. For Raman spectroscopy, it was confirmed the presence of corundum (alumina) phase at characteristic frequencies of 378, 416 and 644 cm^{-1}, hematite phase at 226, 292, 411 and 612 cm^{-1}, magnetite phase at 520 and 668 cm^{-1} and spinel $MgAl_2O_4$ and (Fe, Mg) (Al_2O_4)) with its main frequencies at 406 and 666 major cm^{-1}.

Keywords: Iron ore, gasification, Corrosion phenomena, spinel $MgAl_2O_4$, widmanstätten ferrites.

INTRODUCTION

In recent years, most of worldwide steel industries have been affected through its natural gas-dependent processes, since the use of this fuel is very expensive due to constant increases in the purchase price. This fact has impacted significantly on the profitability of these industries; hence, it was decided to seek other sources of combustible gases, among which mainly use biomass, waste coal and petroleum coke through their gasification process [1-3]. This process has become of great interest in the scientific/technological community, leading to many investigations which have been focused on the use of petroleum coke as a fuel source to produce electricity more cleanly and efficient [4-6]. In a gasification process, usually known as synthesis gas or syngas for short, solid or liquid fuel chemically reacts with a gasification agent (air, oxygen or water vapour) at different temperature ranges depending on the type of the gasifier being used. The most useful way of classifying the gasifiers is by flow regime, i.e. the way in which the fuel and oxidant flow through the gasifier. They may be divided into three basic types groups: entrained flow, fluidised bed and moving bed. General characteristics of each gasifier type as well as characteristics of a new gasification process aimed to the steel making industry (Molten Iron Process "MIP") are listed in Table 1.

The MIP involves three stages: the first one is the reduction of iron ore to produce sponge iron also called DRI (Direct Reduced Iron), which takes place in a direct reduction reactor; the second one is the gasification of petroleum coke with the DRI smelting and takes place in

a gasifier furnace, and the third one is the refining of DRI to produce steel in the Electric Arc Furnace (EAF).

Table 1. Comparison of gasifier types [7- 9].

	Conventional Gasifiers			New Development
	Entrained flow	Fluidised bed	Moving bed	MIP Process
Fuel types	solid and liquid	solid	solid	solid
Fuel size (solid)	<500µm	0.5-5mm	5-50mm	0.5-5mm*
Fuel residence time	1-10s	5-50s	15-30min	1-10s*
Gas outlet temperature	900-1400°C	700-900°C	400-500°C	400-500°C
Gas maximum temperature	~1400°C	~1000°C	~1000°C	~1900°C

*Under investigation

The gasification furnace is the process fulcrum point, since the reducing gases produced here are used in the Direct Reduction Reactor (DRR), and the hot metal obtained inside is the raw material for the EAF. The gasification of petroleum coke (petcoke) is carried out in this furnace to produce reducing gases such as H_2 and CO, see below equation 1, which will be fed into the direct reduction reactor for the production of DRI, see equations 2 and 3 below which will be fed into the gasification furnace to produce high carbon hot metal.

$$\text{Petcoke} + H_2O\ (\text{steam}) + O_2 \rightarrow CO + H_2 + CO_2 + \text{ash} \quad (1)$$

$$Fe_2O_3 + 3CO \longrightarrow 2Fe^{\circ} + 3CO_2 \quad (2)$$

$$Fe_2O_3 + 3H_2 \longrightarrow 2Fe^{\circ} + 3H_2O \quad (3)$$

It is very important to mention that the current gasifiers operate at relatively low temperatures in comparison to that intended to develop in the MIP process. Nevertheless, gasify petroleum coke is not just needed, it is also necessary to smelt the DRI to produce hot metal. To achieve this, as in the Blast Furnace, it is required high flame temperatures. In other words, this equipment is not only a gasifier, such as current reactors, but also a smelter-gasifier.

To implement this innovative technology, it requires the use of high performance refractory materials since operating conditions that involve this technology are very severe, which can result in corrosion phenomena and weakening in the employed refractory. For this reason in this study, exploratory tests were conducted in order to evaluate the chemical interaction and the occurrence of possible reactions between the iron ore (Fe_2O_3) and an Al_2O_3-$MgAl_2O_4$ based refractory concrete (designed and manufactured at laboratory scale). The results in this paper are part of a wider study accomplished by the author on the effects of petroleum coke use as an alternative fuel to natural gas in the iron and steel industry, on the properties of refractory materials [10].

MATERIALS AND METHODS

Raw materials and specimen preparation

The refractory concrete was designed and manufactured in cubes whose dimensions were 50x50x50 mm using two types of materials. The material 1 was constituted for fused alumina, magnesia, magnesium aluminate and the material 2 for fused alumina. After the formulation fabrication, these materials were crushed, grinded and homogenized. Also these materials were characterized by X-ray diffraction (XRD). Later, the refractory concrete was fabricated using a mixing ratio of material l/material 2 = 5.67(85% material 1 / 15% material 2) with a particle size less than 149 µm for both materials, as well as a ratio of 0.25 water / material. However, the particle size was quite different, for material 1 it was in a range between 4.76 mm - 44 µm and for material 2 a grain size equal to 6 mm was used.

The development of the refractory concrete was done as follows: first, the materials were homogenized for 2 min and mixed for 2 min. Then mixtures were casted in molds requiring a vibrated process for 2 min. Later, the refractory concrete was carried out in the shade at 27ºC for 48 hours. Subsequently were stripped and drying at 110°C for 8 hours. Finally, were sintered in a tunnel kiln using air atmosphere, natural gas as fuel and a sintering

temperature of 1720ºC. After the sintering process, a representative sample was characterized by X-Ray Diffraction (XRD), scanning electron microscopy using energy dispersive spectrometry (SEM-EDS) and X-ray fluorescence (XRF).

Corrosion test

The corrosion test in refractory concrete was conducted using a high purity iron ore as a reagent (characterized by XRD). This reagent was compressed to 5mm thick pellet of 12.7 mm in diameter (it took 1 gram of reagent which was isostatically pressed into a stainless steel mold by applying a load of 3 tons). Later a pellet was placed in the center top of the refractory concrete and the whole (refractory-pellet) was subjected to chemical interactions within an electric furnace at 1650 ºC for a period of 4 hours, under atmospheric air, based in the specifications of DIN 1069 for laboratory tests [11]. After the test was conducted, the refractory concrete was sectioned transversely for visual inspection, having as a final objective the evaluation of slag penetration and corrosion attack provoked by slag iron ore. The area with slag penetration was extracted and subjected to characterization by XRD (for which it was crushed, ground and sieved to particle sizes less than 75 μm), SEM-EDX (for which it was embedded in resin, grinded with silicon carbide sandpaper, polished with diamond paste and coated with graphite) and Raman spectroscopy. The Raman Spectra of the refractory concrete was measured by Leica microscope (DMLM) integrated to the Raman system (Renishaw 1000B). The Raman system was calibrated with a silicon wafer using the Raman peak at 520 cm^{-1}. The wavelength of excitation was 830 nm and the laser beam was focused (spot size of approximately 2.0 nm) on the surface of the sample with a x50 objective. The laser power irradiation over the samples was 100 mW. Each spectrum was registered with an exposure time of 30 s, and collected in the 1800–100 cm^{-1} region with 2 cm^{-1} of spectral resolution. In order to determine a profile of inside slag penetration and analysis of possible phases formed, also were characterized by optical microscopy (OM) using dark and bright field.

RESULTS AND DISCUSSION

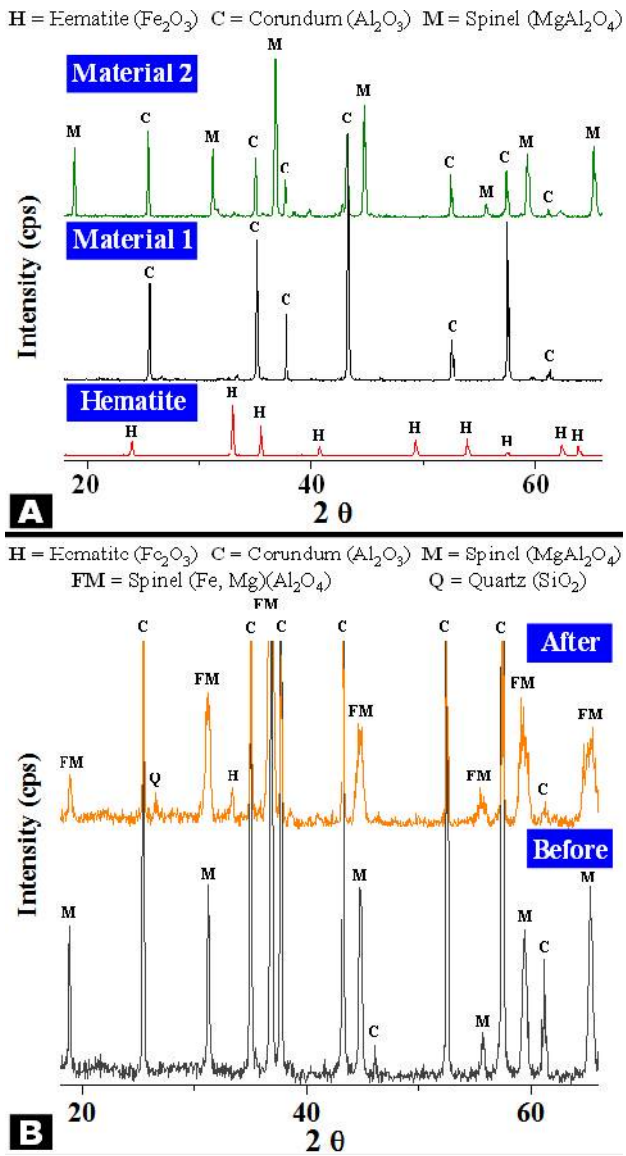

Fig. 1. Phase's analysis by XRD: A) raw materials and B) refractory concrete before and after of the corrosion test.

XRD's for all raw materials are shown in Figure 1A. The phases identified according to the main hkl reflections for iron ore is: hematite phase in characteristics 2Θ 33.052, 35.542 and 53.950; for material 1 are: corundum; for material 2: magnesium aluminate spinel, corundum and periclase; XRD´s for refractory concrete before and after the test are shown in Figure 1B; The mineralogical characterization results for the refractory concrete before the test exhibited mainly the alumina phase and minority magnesium aluminate spinel ($MgAl_2O_4$) phase; after the corrosion test (made in the areas of penetration section corresponds to the attack made with the iron ore), the detected phases in refractory concrete were: corundum, magnesium aluminate spinel ((Fe, Mg)(Al_2O_4)), hematite and quartz (impurities from the grinding process). Regarding the magnesium aluminate spinel phase, it can be observed that the width of the intensities corresponding to this phase was greater after the corrosion test; this is attributed to the incorporation of Fe^{+2} in the initial $MgAl_2O_4$ spinel phase.

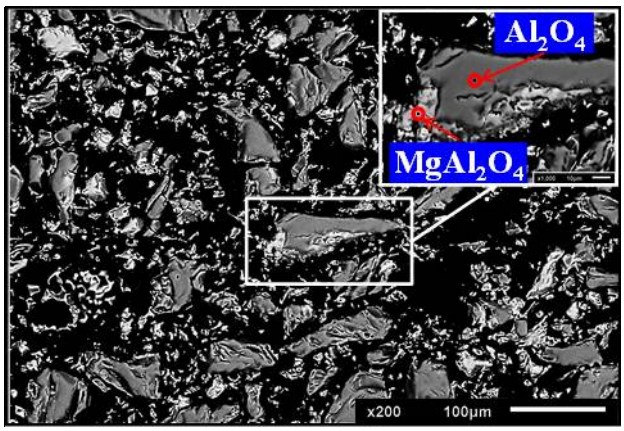

Fig. 2. Microstructural analysis by SEM of the refractory concrete before corrosion test.

Microscopic characterization by SEM of the refractory concrete before the corrosion test is shown in figure 2. In this figure, it can see the presence of alumina and alumina-magnesia spinel grains, which are identified with red circles. The spinel phase is detected around the grains of alumina in a light gray colour.

These phases were corroborated by EDS analysis, whose results are shown in Table 2. In addition, the results obtained by XRF technique are presented also in this table, whose values show that the refractory concrete is made up 70 % by weight of alumina phase and 30 % by weight of magnesium aluminate phase.

Table 2. Chemical analysis by XRF and SEM of refractory concrete before corrosion test.

	XRF (wt.%)								
	Al_2O_3	$MgAl_2O_4$	Fe_2O_3	SiO_2	CaO	Na_2O	Cr_2O_3	-	Total
	67.5	27.92	3.07	1.24	0.22	0.05	0.04	-	100
	SEM (EDS, wt.%)								
	O		Mg		Al		Fe		
Al_2O_3	40.72		-		58.94		0		100
$MgAl_2O_4$	35.17		12.78		47.48		4.57		100

Figure 3 show the refractory concrete-reactive set pellet before and after the test corrosion, as well as the cross-section cut of this set. The affected zone of penetration of molten slag of iron ore, which is identified with red circle, was evaluated to determine the penetration level with the image analyzer SCION IMAGE. The analysis was carried out on images obtained by camera, stereoscopy, optical microscope (OM) and scanning electron microscopy (SEM).

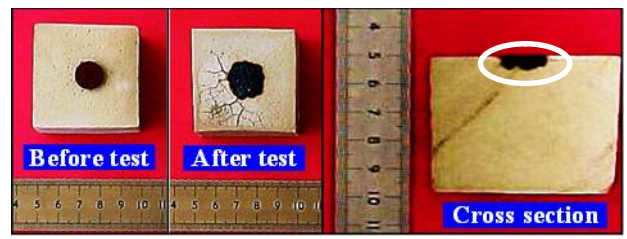

Fig. 3. (A) Reactive pellet / refractory concrete set before the test, (B) Refractory concrete after test and (C) Cross section cut of the set.

The images obtained by these technics are shown in figure 4. Acquisition area was located taking as a reference the contact surface (pellet/refractory

formulation) and the midpoint of the total refractory formulation dimension (marked with a white circle in Figure 3). According to the analysis of penetration level registered by chemical interaction of iron ore with the refractory concrete, it can be observed that there is a penetration depth of 6.24 mm.

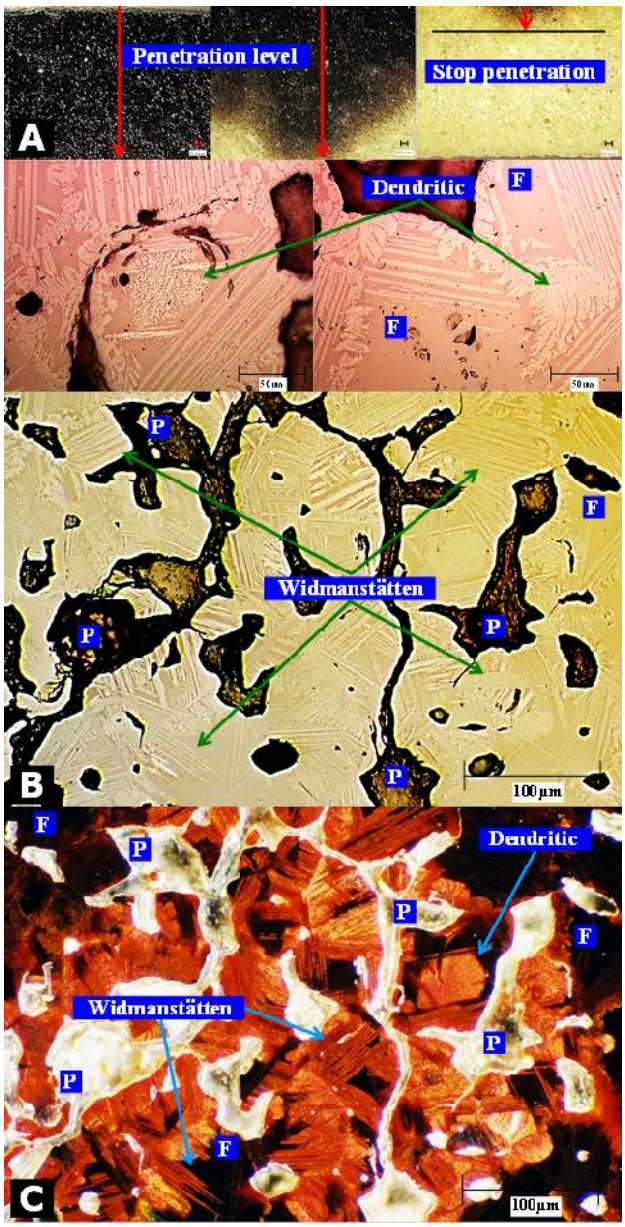

Fig. 4. Microstructural analysis on the refractory concrete after the corrosion test. Images obtained by: A) Stereoscope, B) Bright-field optical microscopy, C) Dark-field optical microscopy.

This value represents less than 50 % of penetration level in comparison with results obtained in another study using the same refractory matrix but in contact with synthetic slag of petroleum coke [12]. This analysis is shown in images of the figure 4A (by Stereoscope and identified by red arrows). On the other hand, in images of the figure 4B obtained by optical microscopy in bright field mode, it can be observed the presence of (Fe, Mg) (Al_2O_4) spinels, which are identified with the letter F, as well as the occurrence of the iron oxide in its three oxidation states (wustite, hematite and magnetite) which occurs as a dendritic and widmanstätten morphologies (both marked with green arrows). Furthermore, in these images the porosity registered in the refractory is marked with the letter "P". Figure 4C shows the image of the refractory concrete analyzed by optical microscopy in dark field mode. In that image, "(Fe, Mg) (Al_2O_4)" spinel phases are identified with the letter F, which corresponds to a black coloration. There is also porosity identified with the letter P, which it is seen in bright white area. Finally, in this image, it can be observed the presence of iron in shades of red color, which is precipitated in dendritic and widmanstätten morphologies and are identified by light blue arrows.

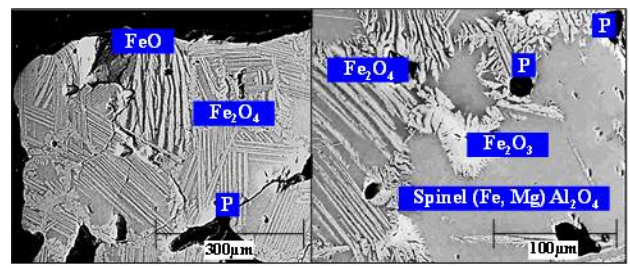

Fig. 5. Microstructural analysis on the refractory concrete after the corrosion test. Images obtained by scanning electron microscopy using backscattered electrons.

The figure 5 showed the microstructural analysis by SEM of the refractory concrete after de corrosion test, in this figure was observed that magnesium aluminate phase incorporates in solid solution Fe^{+2} ions, resulting in the

formation of (Fe, Mg) (Al_2O_4) spinels and after their saturation, the rest of Fe^{+2} ions tended to precipitate at the grain boundaries of alumina and magnesium aluminate phases. This fact promotes during the concrete cooling, the formation of wustite, hematite and magnetite phases (detected in the microstructure as a dendritic and widmanstätten morphologies), which are identified in the images of this figure. In this figure, it was also observed high porosity that is identified as "P".

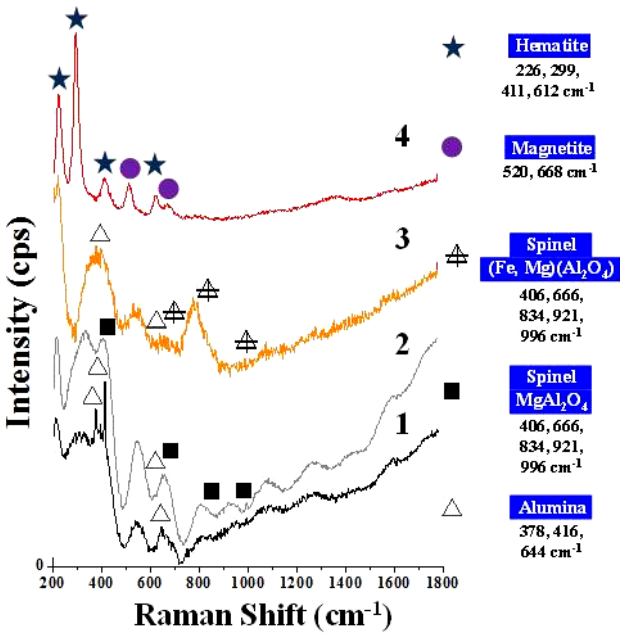

Fig. 6. Results of material characterization by Raman spectroscopy.

Results obtained by Raman spectroscopy technique are shown in figure 6. The Raman spectrum designated as 1, was obtained from the specific analysis carried out in a fused alumina grain, which according to background corresponds to the corundum phase [13], corroborated by characteristic frequencies at 378, 416 and 644 cm^{-1}. The Raman spectrum designated as 2 corroborated the spinel phase $MgAl_2O_4$ [14-15] and (Fe, Mg) (Al_2O_4)) at characteristic frequencies of 406 and 666 cm^{-1}. The specific analysis carried out in microstructural areas where dendritic and widmanstätten morphologies were located (Raman spectrum 4), revealed the presence of hematite phase at 226, 292, 411 and 612 cm^{-1} [16], and magnetite phase at 520 and 668 cm^{-1} [17].

CONCLUSIONS

Through this work, it was concluded that the refractory concrete manufactured is not suitable for operating conditions for which it was designed, since it is susceptible to initial phase dissolution due to the molten slag penetration.

Molten slag generated by the hematite pellet provoked microstructural changes (formation of dendritic and widmanstätten morphologies) and precipitation of new phases such as hematite and magnetite.

Melting points of hematite and magnetite (~ 1600 ° C) are lower than the refractory concrete can tolerate (~ 2100 ° C).

These facts promoted in the refractory concrete an expansive phenomenon that it was reflected as cracking.

REFERENCES

[1] E. Kurkela, M. Kurkela. (2009) "Advanced Biomass Gasification for High-efficiency Power", *BiGPower Project.*

[2] J.C. González-Rocha, R. Longoria-Ramírez, G. Urquiza-Beltran. (2008) "Results of the simulation of gasification on the Mexican petroleum coke from the refineries of Ciudad Madero and Cadereyta" *Ingeniería Investigación y Tecnología* 9: 99-111

[3] Y. Yun, J.S. Ju. (2003) "Operation performance of a pilot-scale gasification/melting process for liquid and slurry-type wastes" *Korean J. Chem. Eng.* 20:1037-1044.

[4] D. Volkmann, C. Reuther, T. Just. (2004) "Refractories for gasification reactors: a gasification technology supplier's point of view", *Refractories Applications and News*. 9:11-8.

[5] S.J. Lee, S.H. Kim, K.H. Kang, Y.D. Yoo, Y. Yun. (2007) "Development of pilot-scale acid gas

removal system for coal syngas" *Korean. J. Chem. Eng.* 24:1128-1132.

[6] Y. Yun, S.W. Chung. (2007) "Gasification of an Indonesian subbituminous coal in a pilot-scale coal gasification system", *Korean J. Chem. Eng.* 24:628-632.

[7] Department of Trade and Industry. (1998) "Gasification of solid and liquid fuels for power generation", *Technology status report, TSR 008.*

[8] W.L. Xiaoting, R. Headrick, S.Z. Dharani. (2005) "Transient stresses in refractory linings of high temperature black liquor gasifier" *Refractories applications transactions* 1:1-8.

[9] T. Nordgreen, T. Liliedahl, K. Sjöström. (2006) "Metallic iron as a tar breakdown catalyst related to atmospheric, fluidized bed gasification of biomass" *Fuel* 85:689-694.

[10] R. Puente-Ornelas. (2005) "Factibilidad de uso de los refractarios Al_2O_3 Y Al_2O_3-$MgAl_2O_4$ en la gasificación de coque de petróleo" Tesis de Maestría, Programa doctoral de Ingeniería en Materiales, FIME-UANL, Nuevo León, México,

[11] German standard DIN 1069: Sicherheitstechnische Anforderungen Und Prüfverfahren.

[12] R. Puente-Ornelas, A.M. Guzman, T.K. Das Roy, G.A. Castillo-Rodriguez, C.J. Lizcano-Zulaica, P.C. Zambrano-Robledo (2010) "Post-mortem study of refractory concretes exposed to corrosive effect of synthetic slag of petroleum coke" *Journal of Materials Science and Engineering* 4 (10):24-33.

[13] Handbook of Raman Spectra. (2000-2002 "Corundum Al_2O_3" *Free database* Laboratoire des Sciences de la Terre ENS-Lyon France.

[14] S.P. Slotznick and S.H. Shim. (2008) "In situ Raman spectroscopy measurements of $MgAl_2O_4$ spinel up to 1400°C" *American Mineralogis* 93:470.

[15] P. Barpanda, S.K. Behera, P.K. Gupta, S.K. Pratihar, S. Bhattacharya. (2006) "Chemically induced disorder order transition in magnesium aluminium spinel" *Journal of the European Ceramic Society* 26 (13):2603-2609.

[16] S.H. Shim and T.S. Duffy. (2001) "Raman spectroscopy of Fe_2O_3 to 62 GPa" *American Mineralogist* 87:318.

[17] F.R. Pérez, C.A. Barrero, K.E. García, A. Hight Walker, J. Tobón, F. Londoño. (2008) "Structural and vibrational characteristics of magnetite as a corrosion product" *Revista Colombiana de Física*, 40 (1):126.